Design of Inhibitors of Orotidine Monophosphate Decarboxylase Using Bioisosteric Replacement and Determination of Inhibition Kinetics

Ewa Poduch,[†] Angelica M. Bello,[†] Sishi Tang,[†] Masahiro Fujihashi,[‡,§] Emil F. Pai,[‡] and Lakshmi P. Kotra*[,†,||]

Molecular Design and Information Technology Center, Leslie Dan Faculty of Pharmacy, University of Toronto, Toronto, Ontario M5S 2S2, Canada, Departments of Biochemistry, Medical Biophysics, and Molecular & Medical Genetics and Division of Cancer Genomics & Proteomics, Ontario Cancer Institute/Princess Margaret Hospital, Toronto, Ontario M5G 2M9, Canada, and Division of Cell and Molecular Biology, Toronto General Research Institute, University Health Network, Toronto, Ontario, M5G 2C4, Canada

Received February 21, 2006

Inhibitors of orotidine monophosphate decarboxylase (ODCase) have applications in RNA viral, parasitic, and other infectious diseases. ODCase catalyzes the decarboxylation of orotidine monophosphate (OMP), producing uridine monophosphate (UMP). Novel inhibitors 6-amino-UMP and 6-cyano-UMP were designed on the basis of the substructure volumes in the substrate OMP and in an inhibitor of ODCase, barbituric acid monophosphate, BMP. A new enzyme assay method using isothermal titration calorimetry (ITC) was developed to investigate the inhibition kinetics of ODCase. The reaction rates were measured by monitoring the heat generated during the decarboxylation reaction of orotidine monophosphate. Kinetic parameters (k_{cat} = 21 s^{-1} and K_M = 5 μM) and the molar enthalpy (ΔH_{app} = 5 kcal/mol) were determined for the decarboxylation of the substrate by ODCase. Competitive inhibition of the enzyme was observed and the inhibition constants (K_i) were determined to be 12.4 μM and 29 μM for 6-aza-UMP and 6-cyano-UMP, respectively. 6-Amino-UMP was found to be among the potent inhibitors of ODCase, having an inhibition constant of 840 nM. We reveal here the first inhibitors of ODCase designed by the principles of bioisosterism and a novel method of using isothermal calorimetry for enzyme inhibition studies.

Introduction

Orotidine monophosphate decarboxylase (ODCase, EC 4.1.1.23) is among the most proficient enzymes known.[1] In human, ODCase is a part of the bifunctional enzyme UMP synthase.[2] In bacteria and parasites, ODCase is a monofunctional enzyme.[3,4] It is involved in the catalytic decarboxylation of orotidine monophosphate (OMP, **1**) to uridine monophosphate (UMP, **2**), which in its triphosphate form is a constituent of RNA as well as a precursor for the synthesis of other pyrimidine nucleotides (Scheme 1). ODCase accomplishes the decarboxylation of OMP without the help of any cofactors and metal ions. This is a remarkable achievement in light of the fact that ODCase (from yeast) exhibits extraordinary rate enhancement of over 17 orders of magnitude compared to the uncatalyzed decarboxylation of orotidine monophosphate in water and at neutral pH, at 25 °C.[1] ODCase is among those few special enzymes that have developed a very high level of sophistication in catalyzing decarboxylation and thus has been a subject of intense investigation.[1,5] Several analogues of OMP have been investigated extensively to understand the catalytic mechanism of ODCase.[6,7] Among these analogues, 6-aza-UMP (**3**) and 6-hydroxy-UMP (or BMP, **4**) are widely known as potent inhibitors of ODCase.[8]

ODCase has been identified as a target for drugs directed against RNA viruses such as poxviruses and flaviviruses; the former are causing increasing concern as a potential bioterrorist weapon.[9−12] ODCase inhibitors have also been effective against West Nile virus, a recent thread to humans and birds in the United States and Canada.[13] Plasmodia, including the malaria-causing *Plasmodium falciparum*, are another class of pathogens sensitive to the inhibition of this enzyme's activity.[14] ODCase has also been evaluated as an anticancer target. Inhibitors of ODCase such as 6-azauridine and pyrazofurin exhibited good anticancer activities against a number of clinical tumor models.[15,16] Moreover, the structures, kinetic profiles, and affinities toward various inhibitors are quite different for ODCase from different sources including yeast, *Escherichia coli*, mouse, *P. falciparum*, and human among others. Thus, ODCase presents itself as a good potential drug target.

Scheme 1. ODCase-Catalyzed Synthesis of Uridine Monophosphate (UMP) from Orotidine Monophosphate (OMP)

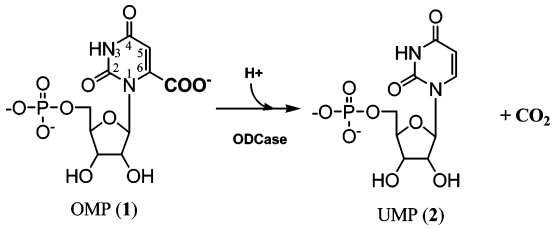

On the basis of the mechanistic understanding of ODCase that a carbon dioxide molecule is eliminated and the resulting anionic center at C-6 is protonated to produce UMP, we designed 6-cyano-UMP and 6-amino-UMP (**5** and **6**, respectively) as potential inhibitors of ODCase (Scheme 1, Chart 1). These two compounds possess small substituents at the C-6 position of the uracil and their size is comparable to that of carboxylate (Figure 1).

Recently in a communication, we revealed that 6-cyano-UMP (**5**) undergoes hydrolysis in the active site of ODCase and generates BMP (**4**).[17,18] The conversion of compound **5** into **4** by ODCase is an unprecedented biochemical event that estab-

* Corresponding author: present address #5-356, Toronto Medical Discoveries Tower, 101 College St., Toronto, Ontario, M5G 2L7 Canada; tel (416) 581-7601; fax (416) 581-7621; e-mail lkotra@uhnres.utoronto.ca.
[†] University of Toronto.
[‡] Ontario Cancer Institute/Princess Margaret Hospital.
[§] Present address: Graduate School of Science, Kyoto University, Sakyo, Kyoto, 606-8502, Japan.
[||] Toronto General Research Institute.

10.1021/jm060202r CCC: $33.50
Published on Web 07/19/2006

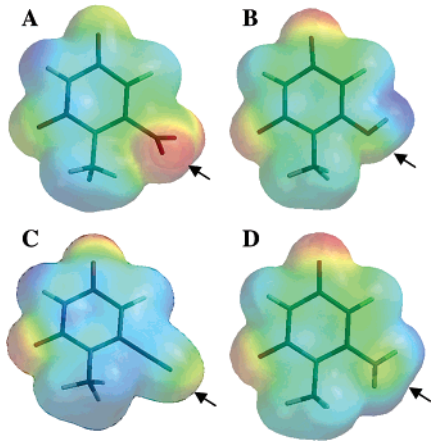

Figure 1. Models of 1-methylorotate (A), 6-hydroxy-1-methyl uracil (B), 6-cyano-1-methyluracil (C), and 6-amino-1-methyluracil (D). Isodensity surface on each model was rendered by use of electrostatic potential (negative charge is represented in red and positive charge in blue). Various substitutions at the C-6 position are shown by the arrow at 5 o'clock position.

Chart 1

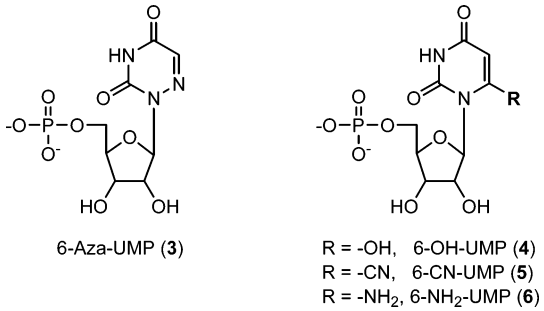

lished its "catalytic" promiscuity for this fascinating enzyme. ODCase converted **5** into **4** very slowly over a period of 24−36 h. It remained unclear if compound **5** itself functions as an inhibitor of ODCase. Here, we reveal the complete details of inhibition kinetics for 6-cyano-UMP (**5**) for the first time. In an effort to conduct enzyme inhibition studies, we discovered that there are no reliable nonradiological assays for ODCase to investigate inhibition profiles. Enzyme assays using ^{14}C-labeled OMP have been used, but the availability of this substrate is an issue for routine enzyme assays. Spectrophotometric assays have been used for ODCase characterization, but when the substrate, inhibitor, and product have overlapping spectral absorption properties (λ_{max}), the spectrophotometric assay is not a method of choice. An alternative nonradioactive method to study ODCase-catalyzed reaction has been proposed by Krungkrai et al.[19] using high-performance liquid chromatography (HPLC).[19] High detection sensitivity (picomolar range) and no need for costly radiolabeled reagents make this method appealing, although the preparation of the sample for HPLC analysis is quite lengthy. The applicability of this method to kinetic investigations of ODCase is limited to monitoring the synthesis of UMP only. The HPLC technique may not be easily adaptable to study enzyme inhibition kinetics. A simple and sensitive method with limited sample preparation and a universal detection system was needed.

Thus, we used isothermal titration calorimetry (ITC) to develop a reliable assay and to study the inhibitory properties. Although ITC is used extensively to study thermodynamic properties of biological systems, including enzymes, this technique has not been explored in-depth to investigate enzyme inhibitions. The recent development of ultrasensitive ITC instruments attracted more attention to this technique as a means to study enzyme inhibition kinetics.[20−22] Isothermal calorimetry's advantages over other commonly used techniques is its ability to detect heat changes during enzymatic reactions under conditions such as poor transparency of reaction solution and free of any chromogenic, fluorogenic, or radioisotope-enriched (labeled) ligands. Heat changes are fundamental in any biochemical event, both during the binding events as well as biochemical reactions; thus ITC is an ideal method for the characterization of enzyme reactions.

Here, we present the details of the design of novel nucleotide inhibitors of ODCase and the determination of enzyme inhibition kinetics by isothermal titration calorimetry assays for the compounds **3**, **5**, and **6**. Findings revealed here set a stage for the design of novel inhibitors of ODCase for probing further details on this enzyme's mechanism as well as novel means to explore enzyme inhibition kinetics in the absence of suitable labeled substrates.

Experimental Section

General. Computer modeling was performed with Spartan version 5.0 software, on an Octane dual processor computer or an Onyx supercomputer at the Molecular Design and Information Technology Center (http://www.phm.utoronto.ca/∼mdit). All synthetic reactions were performed under nitrogen atmosphere. All solvents and reagents were obtained from commercial sources. Chromatographic purifications were performed on silica gel (60 Å, 70−230 mesh) or Dowex (OH^-) ion-exchange resin. NMR spectra were recorded on a Varian spectrometer (recorded at 300 and 400 MHz for ^{1}H, 75 and 100 MHz for ^{13}C, and 121.46 MHz for ^{31}P). Chemical shifts are reported in δ (parts per million, ppm) with tetramethylsilane as a reference for the ^{1}H and ^{13}C spectra, and phosphoric acid as an external standard for ^{31}P spectra. 6-Azauridine was purchased from Aldrich, and other chemicals were either purchased or synthesized from commercially available starting materials. Mass spectra for organic compounds were obtained on a Q-Star mass spectrometer by either the ESI or EI technique. Mononucleotide derivatives were converted into the corresponding ammonium salts by neutralization with 0.5 M NH_4OH solution at 0 °C and freeze-dried to obtain the ammonium salts as powder. For enzymology, orotidine monophosphate trisodium salt (OMP, **1**) and Tris buffer were purchased from Sigma. DL-Dithiothreitol (DTT) was obtained from Fluka Chemicals. *Methanobacterium thermoautotrophicum* ODCase (EC 4.1.1.23) was expressed in *E. coli* and purified as described previously.[23] All ligands used for the calorimetric measurements were prepared as concentrated stock solutions and stored at −20 °C.

Computer Modeling. Models of 6-carboxy-1-methyluracil, 6-hydroxy-1-methyluracil, 6-cyano-1-methyluracil, and 6-amino-1-methyluracil were used as mimics of OMP, BMP (protonated form), 6-cyano-UMP, and 6-amino-UMP, respectively, to understand the effects of the C-6 substitution (Figure 1). Position 1 in these nucleic bases were substituted with a methyl group (in place of a ribos-1-yl 5-monophosphate) and were geometry-optimized with AM1 Hamiltonian as implemented in Spartan version 5.0.[24] The electrostatic potential surfaces were constructed after the geometry optimization of the compounds by mapping the electrostatic property on the isodensity surface. The isovalue was set at 0.002 electron/Bohr^3. The volumes for 1-methyluracil, 6-amino-1-methyluracil, 6-hydroxy-1-methyluracil (protonated species), 6-cyano-1-methyluracil, 6-hydroxy-1-methyluracil (deprotonated species), and 1-methylorotate were 113.59, 141.13, 122.17, 132.68, 114.81, and 140.11 Å^3, respectively. Substructure volumes for 6-carboxylate, 6-hydroxyl, 6-cyano, and 6-amino groups were derived by subtracting the volume of 1-methyluracil from those of the appropriate nucleic base derivatives.

Syntheses: 6-Cyanouridine 5′-*O*-Monophosphate (5). Compound 5 was synthesized as reported earlier.[17]

6-Azido-5′-*O*-(*t*-butyldimethylsilyl)-2′,3′-*O*-isopropylideneuridine (8). Compound **7** (0.25 g, 0.48 mmol) was dissolved in dry *N*,*N*-dimethylformamide (DMF) (3 mL), and NaN_3 (0.034 g, 0.53 mmol) was added. The reaction mixture was stirred at room temperature for 1 h in the dark. Organic solvent was evaporated under vacuum and the crude residue was dissolved in ethyl acetate (15 mL), washed with brine, and dried (Na_2SO_4). Organic layers were evaporated and the crude was purified by silica gel column chromatography (1% EtOH/$CHCl_3$). Purification of the compound and solvent evaporation were performed in the dark to yield the compound **8** (0.19 g, 0.44 mmol) in 92% yield as a light brown solid. ^{1}H NMR ($CDCl_3$) δ 0.06 (s, 6H), 0.89 (s, 9H), 1.34 (s, 3H) 1.54 (s, 3H), 3.74−3.85 (m, 2H), 4.08−4.15 (m, 1H), 4.80 (dd, 1H, J = 4.8 and 6.3 Hz), 5.14 (dd, 1H, J = 1.5 and 6.3 Hz), 5.50 (s, 1H), 6.09 (dd, 1H, J = 1.5 Hz), 9.12 (br s, 1H).

6-Azidouridine (9). A stirred solution of compound **8** (0.300 g, 0.683 mmol) was treated with 50% aqueous trifluoroacetic acid (3 mL) at 0 °C. The reaction mixture was then brought to room temperature and was stirred for an additional hour. Evaporation of the solvent and purification of the crude residue by column chromatography (10−15% EtOH in $CHCl_3$) gave the product **9** (0.17 g, 0.61 mmol) in 89% yield as a light brown solid. UV (H_2O) λ_{max} = 285 nm; ^{1}H NMR (D_2O) δ 3.77 (dd, 1H, J = 5.4 and 12.0 Hz), 3.89−4.00 (m, 2H), 4.43 (t, J = 6.9 Hz, 1H), 4.77 (dd, 1H, J = 3.6 and 6.9 Hz), 5.76 (s, 1H), 6.07 (d, 1H, J = 3.6 Hz). HRMS (ESI) calcd for $C_9H_{11}N_5O_6Na$ ($M + Na^+$) 308.0601, found 308.0597.

6-Aminouridine 5′-*O*-Monophosphate (6). A stirred solution of water (0.03 g, 1.89 mmol) and $POCl_3$ (0.28 mL, 2.97 mmol) in anhydrous acetonitrile (3 mL) was treated with pyridine (0.26 mL, 3.24 mmol) at 0 °C and stirred for 10 min. Compound **9** was added (0.25 g, 0.68 mmol) and the mixture was stirred for an additional 5 h at 0 °C. The reaction mixture was quenched with 25 mL of cold water and the stirring was continued for another hour. Evaporation of the solvent and purification of the crude by column chromatography (Dowex ion-exchange basic resin, 0.1 M formic acid) gave the mononucleotide (0.23 g, 0.63 mmol) in 60% yield as syrup. UV (H_2O) λ_{max} = 283 nm; ^{1}H NMR (D_2O) δ 3.78−3.85 (m, 1H), 3.89−4.00 (m, 2H), 4.34 (t, J = 6.9 Hz 1H), 4.80 (m, 1H), 5.73 (s, 1H), 6.04 (br s, 1H). ^{31}P NMR (D_2O) δ (ppm) 2.47. HRMS (ESI, negative) calcd for $C_9H_{11}N_5O_9P$ (M^-) 364.0299, found 364.0307.

The mononucleotide (0.06 g, 0.15 mmol) was then dissolved in 50% aqueous methanol and 10% Pd/C (10 mg) was added. The reaction mixture was stirred for 2 h under hydrogen atmosphere at room temperature. The mixture was filtered through Celite and the solvent was evaporated to dryness to give compound **6** as syrup in 85% yield (43 mg, 0.13 mmol). UV (H_2O) λ_{max} = 270 nm; ^{1}H NMR (D_2O) δ 3.96−4.05 (m, 2H), 4.12−4.24 (m, 2H), 4.51 (t, J = 6.6 Hz, 1H), 4.81 (s, 1H), 6.20 (d, J = 6.6 Hz, 1H). HRMS (ESI, negative) calcd for $C_9H_{13}N_3O_9P$ (M^-) 338.0394, found 338.0403.

6-Azauridine 5′-*O*-Monophosphate (3). A stirred solution of water (0.034 g, 1.89 mmol) and $POCl_3$ (0.28 mL, 2.97 mmol) in anhydrous acetonitrile (3 mL) was treated with pyridine (0.261 mL, 3.24 mmol) at 0 °C and stirred for 10 min. Compound **10** (0.200 g, 0.81 mmol) was added and the mixture was stirred for an additional 5 h at 0 °C. The reaction mixture was quenched with 25 mL of cold water and stirring was continued for an additional hour. Evaporation of solvent and purification of the crude by column chromatography (Dowex ion-exchange basic resin, 0.1M formic acid) gave the mononucleotide **3** (0.17 g, 0.51 mmol) in 63% yield as a syrup. UV (H_2O, pH = 6) λ_{max} = 260 nm; ^{1}H NMR (D_2O) δ 3.85−4.07 (m, 3H), 4.33 (t, J = 5.7, 1H), 4.46 (dd, 1H, J = 3.0 and 5.1 Hz), 5.96 (d, 1H, J = 3.0 Hz), 7.46 (s, 1H). ^{31}P NMR (D_2O) δ 0.55. MS (ESI, negative) *m*/*z* 342 ([MNH_4]$^-$, 100), 324 (M^-, 62), 404 ([M2K]$^-$, 30).

Isothermal Titration Calorimetry and Enzyme Kinetics. The thermal power (microcalories/second) is directly proportional to the rate of the reaction (R_t). This relationship allows derivation of kinetic parameters (k_{cat} and K_M), and molar enthalpy (ΔH_{app}) in a single experiment:[25]

$$\text{power } (P) = \frac{dQ}{dt} \tag{1}$$

If one were to measure the heat from a biochemical reaction, the amount of net heat (Q_{net}, simply shown here as Q) generated or absorbed during the conversion of n moles of substrate into product is expressed by

$$Q = n\Delta H_{app} = [P]_t V_0 \Delta H_{app} \tag{2}$$

where, ΔH_{app} is molar enthalpy, $[P]_t$ is the concentration of the product generated, V_0 is the volume of the ITC cell (1.3 mL). Upon rearrangement of eq 2, a relationship between the rate of change in the product concentration, the molar enthalpy, and the thermal power is obtained:

$$\text{power } (P) = \frac{dQ}{dt} = \frac{d[P]_t}{dt} V_0 \Delta H_{app} \tag{3}$$

To determine ΔH_{app}, the total heat (Q) generated by the reaction is divided by the number of moles of substrate (n) converted into product[22] (assuming complete substrate depletion). Reaction rate at time t is calculated from eq 4 and is plotted as a function of [S]:

$$R_t = \frac{d[P]_t}{dt} = \frac{1}{V_0 \Delta H_{app}} \frac{dQ}{dt} \tag{4}$$

V_0 is the volume of the sample cell, which is a constant, and Q and t are values measured during the experiment. ΔH_{app} is calculated as described above. Substrate concentration $[S]_t$ at any instance t is determined from

$$[S]_t = [S]_{t=0} - \frac{\int_0^t P\, dt}{V_0 \Delta H_{app}} \tag{5}$$

where $[S]_{t=0}$ is the initial substrate concentration.[26]

By use of the enzyme concentration [E], the catalytic rate k_{cat} and the Michaelis constant K_M can be determined by fitting $[S]_t$ and R_t to the Michaelis−Menten equation:

$$v = \frac{k_{cat}[E][S]_t}{K_M + [S]_t} \tag{6}$$

In the presence of inhibitor, the rate is calculated by fitting the data to the competitive inhibition equation:

$$v = \frac{k_{cat}[E][S]_t}{K_M\left(1 + \frac{[I]}{K_i}\right) + [S]_t} \tag{7}$$

The inhibition constant (K_i) is the only fitting parameter, and the values of k_{cat}, K_M, ΔH_{app}, and [I] (determined from separate experiments) are used as variables.[26]

Enzymology. The substrate OMP (**1**) solution was prepared with dialysis buffer (vide infra) as a concentrated 20 mM stock solution and diluted as required. The OMP (**1**) stock solution was stored in aliquots at −20 °C. Concentrated solutions of all inhibitors were prepared in the same buffer as the substrate and the enzyme.

The enzyme was dialyzed against Tris buffer (50 mM Tris, pH 7.5) by use of DiaLyzer dialysis cassettes (MW cutoff 10 000) from Pierce. The reaction buffer for ITC experiments was prepared with triple-distilled water. ODCase samples for each assay were prepared by diluting enzyme stock solution with Tris buffer supplemented with DTT (1 mM final concentration). Substrate and inhibitors were dissolved in the buffer collected from the dialysis, to maintain homogeneity between the buffers used for the enzyme and the ligands. Prior to the injections in the microcalorimeter, enzyme and

ligand samples were degassed with stirring for 5 min by use of a vacuum degasser (ThermoVac, MicroCal). The degassed solution was transferred to the sample cell via a gastight Hamilton syringe.

Experimental Conditions. All enzyme reactions were performed at 55 °C, the optimal growth temperature of *M. thermoautotrophicum*. Titrations were performed on an isothermal titration calorimeter, VP-ITC instrument from MicroCal (Northampton, MA). In all cases, the calorimetric cell contained the enzyme solution while the ligand(s) were loaded into the automatic injection syringe. The reference cell was filled with degassed reaction buffer. In the case of control reaction (without inhibitor), the syringe contained the substrate OMP (**1**) only. Substrate and inhibitor mixtures were prepared and loaded into the injection syringe to monitor enzyme activity in the presence of inhibitor. The concentrations of the substrate and inhibitor in the syringe were calculated to give the desired, final concentration of each component in the calorimetric cell after one injection. Single injection method was used in all studies. Substrate was injected into the enzyme solution in a single injection, and change in heat was measured as the reaction progressed until the heat returned to baseline, indicating the end of the reaction. After the preliminary equilibration period when the instrument reached the final temperature of 55 °C, an additional 60 s delay period was allowed to generate the baseline used in the subsequent data analyses. After a 60 s delay, each reaction was automatically initiated by a 20 μL injection of ligand into the enzyme-containing cell. The stirring rate of the injection syringe was set to 300 rpm. Heat flow (microcalories/second) was recorded as a function of time. Data were collected every 2 s until the signal reached the baseline and continued to be recorded for an additional 60−100 s to generate the final baseline. The time of reaction varied from 5 to 25 min depending on the type of assay (i.e., enzyme activity or inhibition assay).

Substrate Catalysis. The rate of OMP decarboxylation at 55 °C was measured in 50 mM Tris buffer at pH 7.5. The reaction was initiated by an injection of 20 μL of substrate (OMP, **1**) into the enzyme solution, and the change in thermal power was monitored until the signal returned to baseline values. The enzyme concentration in the cell was 20 nM and the substrate concentration in the syringe was 2.86 mM (after injection, the final concentration of the substrate was 40 μM in the reaction cell). The reaction rate was also determined at 25 °C with 20 nM and 100 nM enzyme. The effective substrate concentration was the same as that in the assay above at 55 °C.

Enzyme Inhibition. Inhibitory properties of the compounds **3**, **5**, and **6** were evaluated by the competitive inhibition method. Mixtures of substrate and each inhibitor were prepared as a concentrated solution to obtain desired dilutions in the calorimetric cell after a 20 μL injection of the mixture. The final OMP concentration was always 40 μM, unless specified otherwise. Final concentrations of each inhibitor in the reaction cell were 10, 25, and 50 μM for compound **3**; 25, 50, 75, and 100 μM for compound **5**; and 0.5, 1.0, 1.5, and 2.5 μM for compound **6**. Enzyme activity was monitored after the addition of the mixture of substrate and inhibitor. The velocity of the reaction without the inhibitor (control) was also measured. Reactions were performed in triplicate. The inhibition constant for 6-aza-UMP (**3**) was calculated by two methods. First, direct fitting of the data from inhibition assays was performed by use of the fitting function in Origin software. In the second method, K_i was derived from the Dixon plot for competitive inhibition (Figure 3C).[27] Fitting of data from the inhibition assay with 6-cyano-UMP (**5**) with Origin software did not yield a good fit. The Dixon method was used instead to derive the inhibition constant for this compound (Figure 4C). K_i for 6-amino-UMP (**6**) was determined by nonlinear least-squares fit of the experimental data to the competitive inhibition equation in Origin 7.0 software.[26]

Compound **5** was also evaluated by ITC against ODCase (*M. thermoautotrophicum*) for its potential time-dependent, tight binding inhibition due to the conversion of **5** into **4**.[17] Samples of ODCase with and without compound **5** were incubated at room temperature, and the enzyme activity was measured by ITC at different time increments as described above. The enzyme concentration in the incubation mixtures was 50 μM, and the concentration of compound **5** was either 25 or 62.5 mM. The final enzyme concentration in the reaction mixture was 20 nM, and the inhibitor concentrations were 10 and 25 μM. Separate control samples without the inhibitor were prepared for each of the two experiments. Reaction mixtures were prepared in 50 mM Tris buffer containing 10 mM DTT and 80 mM NaCl. Enzyme activity was measured after 1-μL aliquots of each sample were diluted to 2.5 mL with the reaction buffer (50 mM Tris and 1 mM DTT, pH 7.5). Each reaction was initiated by the addition of 20 μL of 2.86 mM OMP. Enzyme activity remaining in the samples containing inhibitor was calculated as a percentage of control activity. The activities in each sample were derived from the slopes of the linear portion of the reaction progress curves.

Data Analysis. Analyses of the raw data were performed with Origin version 7.0 software.[26] Baseline data points before the injection and after the completion of reaction were removed prior to any calculations. The data representing the heat of substrate dilution and mixing were not considered in the data analyses. The remaining data represent the reaction progress curve (Figure 2A). These curves were analyzed in Enzyme Assay mode in Origin software. The reaction progress curves at specific substrate concentrations were considered for further analyses and data fitting. Kinetic parameters (K_M and k_{cat}) as well as the enthalpy for the reaction of OMP decarboxylation were calculated by use of Origin version 7.0 software. Direct determination of K_i values with this software was performed by nonlinear squares fit of the data to the competitive inhibition equation (eq 7) with K_M, k_{cat}, and ΔH_{app} as fitting variables determined in the absence of inhibitor.

Another method employed to derive the inhibition constant (K_i) is by converting raw data from inhibited reactions to Michaelis−Menten curves by use of the Substrate Only mode in the Origin software to fit the raw data. This allowed for the computation of the reaction rates at each substrate concentration in the absence and presence of inhibitor. Since the reaction times ranged from 5 to 25 min, there was a large number of data points (collected every 2 s). Several substrate concentrations, spanning the length of the Michaelis−Menten curve (Figure 3B vs 4B), were selected for subsequent data analysis (Figure 3B). The same set of substrate concentrations and the corresponding reaction rates were selected from each experiment. The inhibition constant was then derived from a Dixon plot by plotting the reciprocal of the reaction rate versus inhibitor concentrations. The value of the inhibition constant, K_i, was determined as the point on the negative x-axis directly below the intersection of the slopes.

Results and Discussion

A survey of known inhibitors of ODCase revealed that BMP (6-hydroxy-UMP or barbituric acid monophosphate) is the most potent inhibitor known to date with a picomolar inhibition constant against yeast ODCase.[8] BMP inhibits yeast ODCase with a K_i of 8.8×10^{-12} M.[8] We were interested in exploring alternate substitutions at the C-6 position using the principles of bioisosteric replacement and the size of the substitution. Thus, we used the structures of OMP, the substrate for ODCase with a carboxyl substitution at the C-6 position, and BMP, the most potent inhibitor of ODCase with a hydroxyl substitution, to compare the characteristics of these substitutions. Both substructures carry a net negative charge and are comparable in size. Upon investigation of the binding site of ODCase, it appears that the space available for a C-6 substitution is not large and should be within the volume limits dictated by the known substrates and inhibitors of ODCase. We decided to use the volumes of the substructures at the C-6 position as a means to design novel inhibitors.

1-Methyluracil, 6-hydroxy-1-methyluracil (representing the protonated form of orotate), 6-cyano-1-methyluracil, 6-amino-1-methyluracil, and 6-carboxy-1-methyluracil were used as model systems for UMP (**2**), BMP (**4**), 6-cyano-UMP (**5**),

Scheme 2[a]

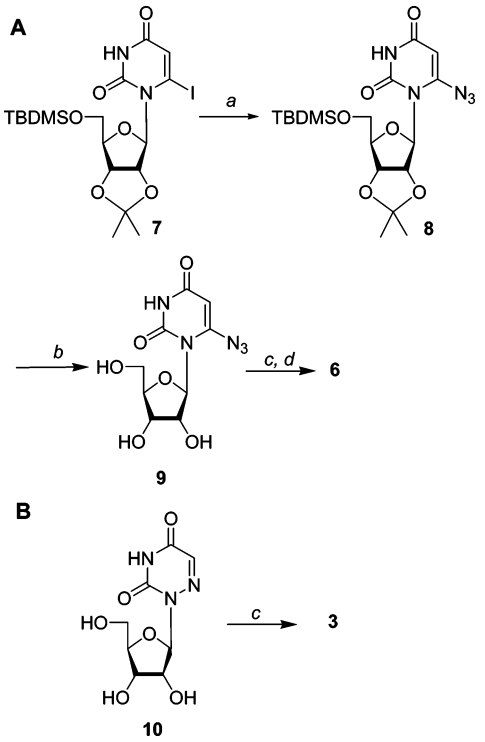

[a] Reaction conditions: (a) NaN_3, DMF, room temperature; (b) 50% TFA, room temperature; (c) $POCl_3$, pyridine, H_2O, CH_3CN, 0 °C; (d) H_2, Pd/C, MeOH, room temperature.

6-amino-UMP (**6**), and OMP (**1**), respectively, to compare the volumes of the substructures at the C-6 position. The substructure volumes for the 6-carboxyl and 6-hydroxyl (protonated form) moieties were 26.5 and 8.6 Å^3, respectively, and these substitutions represent the volumes in the substrate OMP and the most potent inhibitor, BMP. In fact, the volume of the deprotonated 6-hydroxyl substitution, which is the most abundant form, is merely 1.2 Å^3 larger than that of the unsubstituted 1-methyluracil. In terms of the inhibitory potency, UMP is a very poor inhibitor of ODCase compared to BMP, despite such small differences in the volume of substitutions. This led to the reasoning that the negative charge at the C-6 position on BMP plays a very important role in enhancing its affinity to ODCase. Thus, our focus has been to incorporate these tight volume limits in the design of a substitution at the C-6 position to create inhibitors of ODCase. On the basis of this information, we decided to investigate 6-cyano and 6-amino groups as potential substitutions on UMP, and their corresponding substructure volumes were 19.1 and 27.5 Å^3, respectively. Thus, compounds **5** and **6** were synthesized as potential inhibitors of ODCase.

Compound **5** was synthesized from uridine according to the previously published report.[17] Compound **6** was synthesized from the 6-iodo derivative **7** (Scheme 2). Introduction of the iodo moiety at the C-6 position of fully protected uridine was achieved through LDA and iodine, and further substitution of the iodo by the azido group produced the 6-azido derivative **8**.[28] Deprotection of the isopropylidene and *tert*-butyldimethylsilyl groups by use of trifluoroacetic acid yielded compound **9**. Monophosphorylation of **9** with phosphorus oxychloride to afford its mononucleotide followed by the reduction of the azido group with Pd/C gave the target compound **6** in good yield.[29−31] The 6-azauracil derivative **3** was synthesized by subjecting **10** to phosphorus oxychloride conditions generating the target mononucleotide. Mononucleotides (free forms) of compounds **3** and **6** were transformed into the corresponding ammonium salts by neutralizing with 0.5 M NH_4OH solution followed by freeze-drying to obtain the corresponding ammonium salt.

ITC has been rarely used to investigate enzyme inhibition profiles, although it found extensive applications in enzyme kinetics and binding studies. Typically, in an isothermal calorimetry experiment, the energy (ΔH) for the association of a protein and its ligand are in the range of 1−25 kcal/mol depending on the experimental conditions.[32−35] Since the heat (Q) is directly related to the concentration of protein (M_{tot}),[36] the assumption made above to use the linear region of the thermogram to interpret enzyme kinetics is reasonable:

$$Q = \Delta H M_{tot} V \tag{8}$$

where Q is heat (microcalories), ΔH is enthalpy (calories/mole), M_{tot} represents total concentration of protein in the cell, and V is the volume of the calorimetric cell. The average enthalpy (ΔH) produced by various ligands binding to ODCase was in the range of 0.5−1.0 kcal/mol, in our experiments, and the concentrations of the ligands and enzymes are in either micromolar or millimolar range. 6-Aza-UMP (**3**, 35 μM final concentration) produced 0.98 kcal/mol corresponding to 49 μcal of heat/injection in the presence of equimolar ODCase (35 μM final concentration) (Figure S-1A, Supporting Information). Compound **5** (final concentration 122 μM after first injection) upon titration with ODCase (50 μM final concentration) produced a total of 0.62 kcal/mol (ΔH), and the corresponding heat (Q) for this reaction was 111 μcal (Figure S-1B, Supporting Information). This enthalpy and the corresponding heat are a result of the first injection in the thermogram. It should be noted that the binding enthalpies (ΔH) for 6-aza-UMP and 6-cyano-

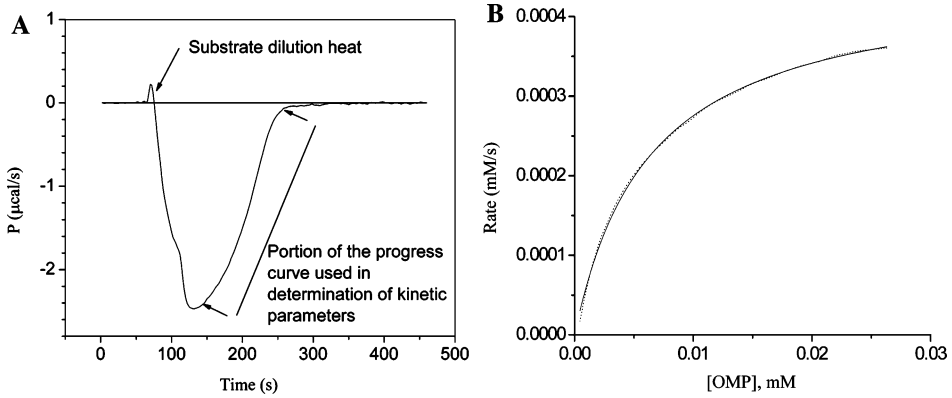

Figure 2. (A) Thermal power change as a function of time during the conversion of 40 μM OMP to UMP catalyzed by ODCase. Reaction was initiated by injection of 20 μL of 2.86 mM OMP into 20 nM enzyme. (B) Nonlinear least-squares fit (solid line) of experimental data (dotted line) to Michaelis−Menten equation to determine kinetic parameters of the ODCase reaction.

Table 1. Kinetic Parameters of ODCase

compound	method	ODCase source	K_m ($\times 10^{-6}$ M)	k_{cat} (s^{-1})	k_{cat}/K_m ($M^{-1}\ s^{-1}$)	ref
OMP at 55 °C	ITC	Mt[a]	5 ± 1	21	4.2×10^6	
OMP at 25 °C	ITC	Mt	2	2	1×10^6	
OMP at 25 °C	UV, radioactivity	Sc[b]	0.7*	42	6×10^7	40, 41
OMP at 25 °C	UV	Pf[c]	13 ± 1	7.5	5.6×10^5	14

[a] *Methanobacterium thermoautothropicum.* [b] *Saccharomyces cerevisiae.* [c] *Plasmodium falciparum.*

UMP were obtained in the presence of 14 and 50 μM ODCase, while enzyme kinetics experiments required only 20 nM enzyme in the reaction cell, or the protein concentration was lower by approximately 3 orders of magnitude.

Considering the sensitivity of the VP-ITC instrument (0.1 μcal) and the direct relation between the binding heat and the protein concentration (eq 8), the heat generated by ligand binding to 20 nM ODCase enzyme would be well below the instrument's detection limits.[36] In fact, we were unable to record any heat exchange due to the presence of inhibitors **3** and **5**, when the enzyme concentration was less than 1 μM. Energies involved in bond breaking/making are several orders of magnitude higher; thus such heats could be used in enzyme kinetics. Monitoring enzyme kinetics and inhibitions as reported here is a feasible means to study various enzyme inhibitors by ITC.

Initially, optimal concentrations of the enzyme and the substrate were determined for the conversion of OMP to UMP by ODCase via ITC. Figure 2A shows a typical thermogram representing heat flow as a function of time for the ODCase-catalyzed reaction. The initial trace from 0 to 60 s represents the baseline, followed by a small peak formed due to substrate dilution effect after the injection of the substrate (Figure 2A). Negative thermal power (P) after the substrate injection indicated that the reaction is exothermic. Maximum heat was released at about 120 s and the signal returned gradually to the baseline almost in a linear fashion after the substrate was consumed, indicating the end of the reaction. The linear portion of the curve was used in the subsequent data analyses (defined by two arrows in Figure 2A). The average time required to catalyze the conversion of 40 μM OMP into UMP at 55 °C was 5 min.

On the basis of the profile in Figure 2A, rates of the reaction at various substrate concentrations were calculated by nonlinear least-squares fit to the Michaelis−Menten equation (eq 6). The output of this calculation is shown in Figure 2B. The Michaelis constant K_M for the *M. thermoautotrophicum* ODCase reaction was 5 ± 1 μM and the catalytic rate constant (k_{cat}) was 21 ± 2 s^{-1} (Table 1). The enthalpy (ΔH_{app}) of conversion of 40 μM OMP to UMP was 5.0 ± 0.5 kcal/mol. The rate of catalysis (k_{cat}) for ODCase from *M. thermoautotrophicum* at 25 °C was 2 s^{-1}, noticeably lower than that at 55 °C (Table 1). The reaction took significantly longer to complete (25 min) but enthalpy (ΔH_{app}) and the K_M were similar to those at 55 °C, as expected. The increase of enzyme concentration from 20 to 100 nM was required to achieve a comparable reaction time (5 min) at 25 °C to the one at 55 °C and the k_{cat} remained at 2 s^{-1}.

Kinetic parameters determined with the thermophilic ODCase by ITC conform to those obtained by a standard UV-based assay where k_{cat} was established to be 42 s^{-1} and 5.4 s^{-1} at 55 °C and 25 °C, respectively.[23] The Michaelis−Menten constant K_M for the same protein was determined as 10 μM.[23] The K_M (5 μM) assessment by the ITC method is also in good agreement with the K_M values determined for ODCase originating from other organisms (Table 1).[37−39] Comparison of the ODCase reaction rates at 25 and 55 °C yielded significantly different values. The discrepancy is characteristic to thermophilic organisms.[40] Thus, the congruence between the ODCase kinetics

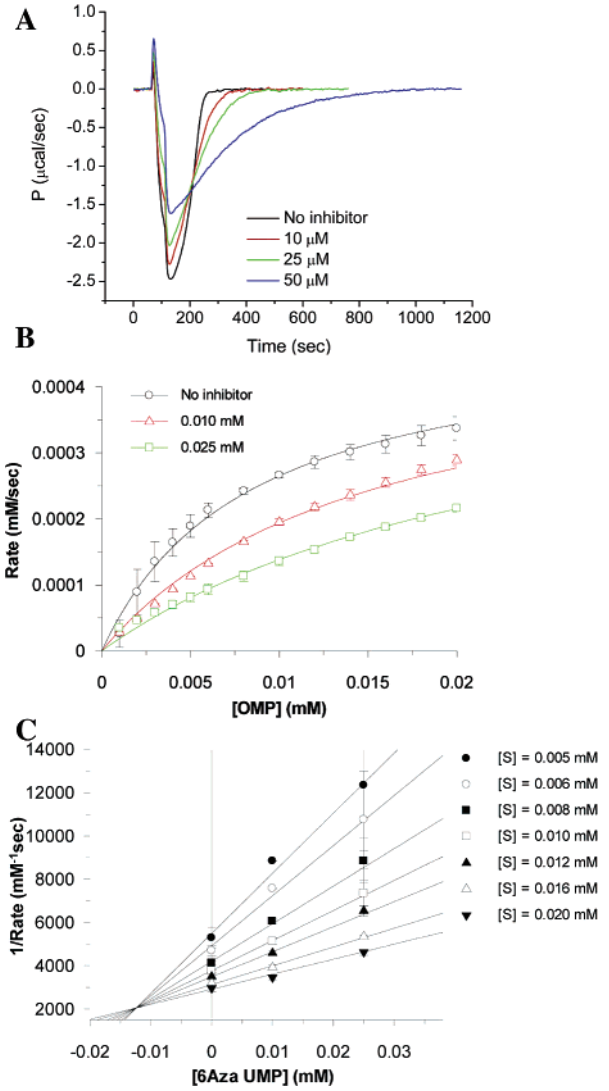

Figure 3. (A) Reaction progress curves in the absence and presence of different concentrations of 6-Aza UMP. (B) Rate of reaction at different substrate concentrations in the presence of 10 and 25 μM 6-Aza UMP. (C) Determination of inhibition constant for 6-Aza UMP from Dixon plot.

measurements with ITC and other known methodologies imparted confidence into this method, and we proceeded to investigate the inhibition kinetics.

Competitive inhibition experiments were performed by injecting substrate and each inhibitor (**3**, **5**, or **6**) simultaneously into the enzyme solution. The inhibitor concentration was varied while the concentrations of enzyme and substrate were kept constant. Figures 3A, 4A, and 5A depict the thermograms generated during OMP decarboxylation in the presence of the inhibitors 6-aza-UMP (**3**), 6-cyano-UMP (**5**), and 6-amino-UMP (**6**), respectively. As the inhibitor concentration was increased, the thermograms exhibited a shallow elongated shape, indicating the presence of fewer enzyme molecules available to catalyze the reaction (thus taking a longer time to complete the reaction).

Table 2. Inhibition Constants for Various Inhibitors of ODCase

compound	ODCase source	K_i (M)	ref
6-aza-UMP (**3**) at 55 °C	Mt[a]	12.4×10^{-6}	
6-aza-UMP (**3**) at 25 °C	Sc[b]	64×10^{-9}	40, 41
6-aza-UMP (**3**) at 25 °C	Pf[c]	1.0×10^{-6}	14
BMP (**4**) at 25 °C (radiolabeled)	Sc	8.8×10^{-12}	8
6-cyano-UMP (**5**) at 55 °C	Mt	$(29 \pm 2) \times 10^{-6}$	
6-amino-UMP (**6**) at 55 °C	Mt	$(840 \pm 25) \times 10^{-9}$	

[a] *Methanobacterium thermoautothropicum*. [b] *Saccharomyces cerevisiae*. [c] *Plasmodium falciparum*.

More heat was needed to balance the temperature differences between the sample and reference cells, resulting in less negative power with increasing inhibitor concentrations.

The "intersecting" nature of the linear regions of thermograms after the completion of the injection prompted us to take a closer look at these curves and explore their use for the interpretation of enzyme inhibition kinetics (Figures 3A, 4A, and 5A). If one assumes that the power compensation imparted by ITC (*y*-axis) during the enzymic reaction is dominated by the heat generated from the enzymatic reaction, and the linear regions in the thermograms reflect the "steady-state" conditions, these curves depict the response of the reaction rate due to various inhibitor concentrations as a function of time. Rate of reaction can be replotted against substrate concentration at various concentrations of the inhibitors to extract inhibition constants (Figure 3B and 4B). On the basis of these assumptions and observations, we interpreted the isothermal calorimetry data to understand the enzyme inhibition profiles.

Initially, we considered a known inhibitor of ODCase, 6-aza-UMP (**3**), and investigated its inhibition of *M. thermoautotrophicum* ODCase. The interactions of 6-aza-UMP with the thermophilic ODCase were studied at 55 °C in a competitive binding assay. Figure 3A shows the profiles of the heat flow (*P*) during the enzymic reaction as a function of time at different concentrations of 6-aza-UMP. Upon replotting of the linear regions from the thermograms in terms of the rate of the reaction versus substrate concentration, a decrease in the enzymic reaction rate was observed as the inhibitor concentration was increased (Figure 3B). By the method of Dixon, the inhibition constant K_i was estimated to be 12.4 ± 0.7 μM for 6-aza-UMP against *M. thermoautotrophicum* ODCase at 55 °C (Figure 3C, Table 2).[27] We also used a nonlinear fitting function in the Origin software and arrived at a K_i of 11 ± 2 μM, confirming the value from the Dixon plot.[26] 6-Aza-UMP is a well-known inhibitor of ODCase with $K_i = 6.4 \times 10^{-8}$ M (yeast enzyme, Table 2).[8,41,42] There is a difference of 2 orders of magnitude in the inhibition constant K_i for ODCase from *M. thermoau-*

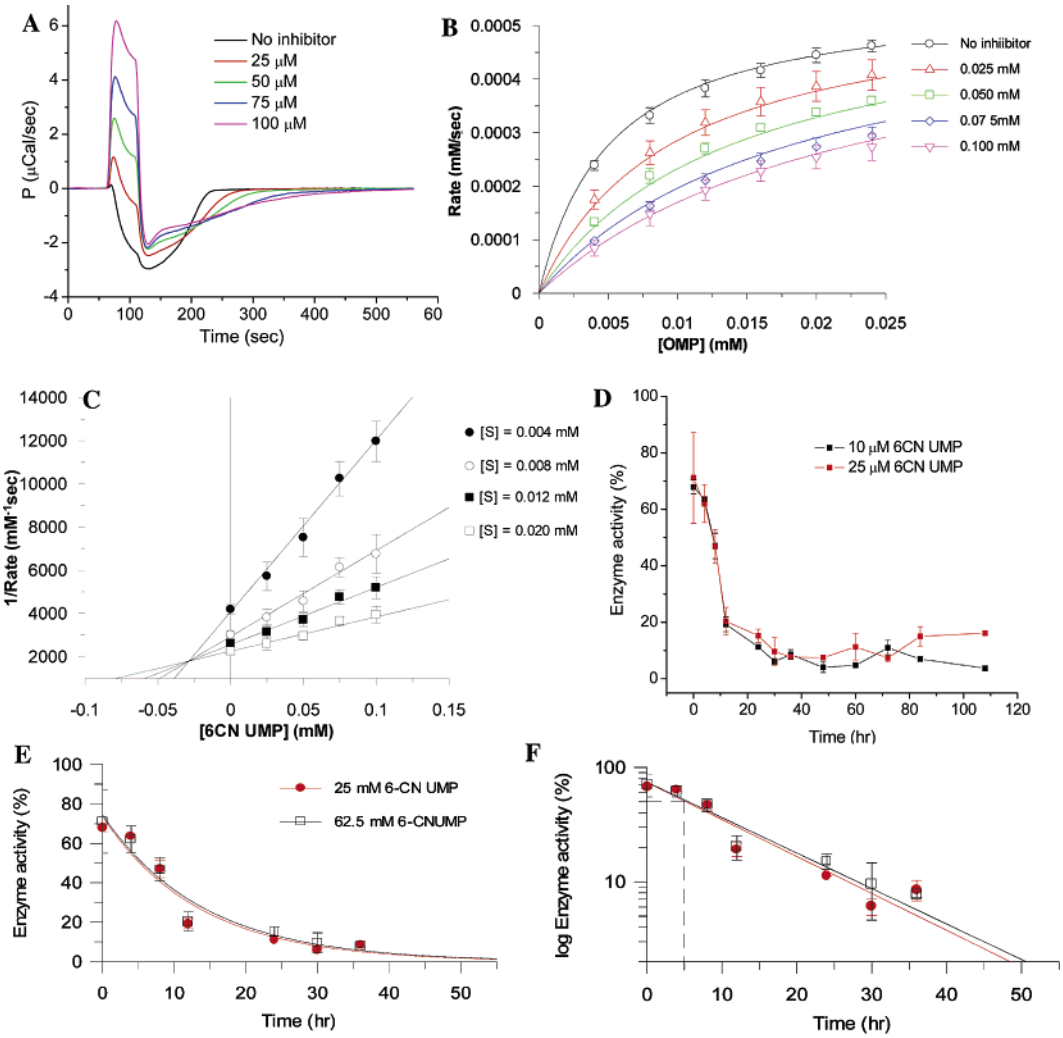

Figure 4. (A) Thermograms for the enzymatic conversion of OMP to UMP in the presence of different concentrations of **5**. (B) Michaelis−Menten curves representing the reaction rates at various substrate concentrations in the presence of **5**. (C) Determination of the inhibition constant, K_i. (D) Time-dependent enzyme activity as a function of time, when the enzyme (20 nM) was incubated in the presence of **5**. (E, F) Time required to inactivate 50% of ODCase activity ($t_{1/2}$) by **5** via its conversion into BMP (**4**) by ODCase.

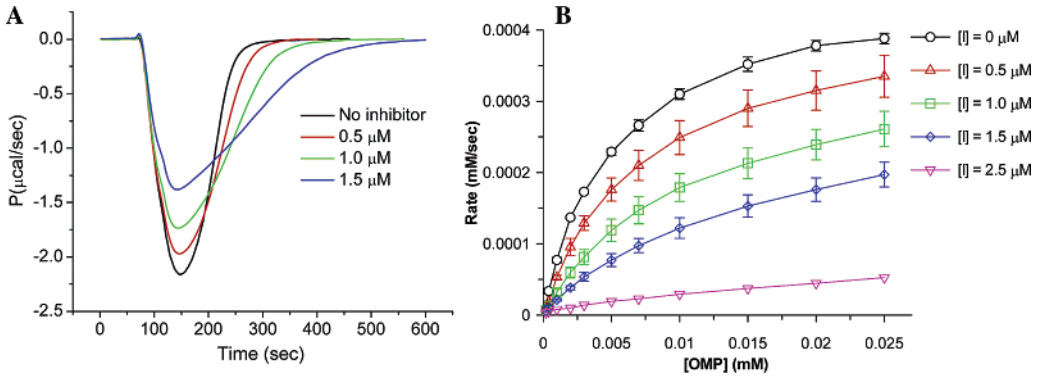

Figure 5. (A) Thermograms of the ODCase reaction in the presence of different concentrations of 6-amino-UMP (**6**) as a function of time. (B) Reaction rate at various substrate concentrations in the absence and presence of inhibitor.

totrophicum and that from *Saccharomyces cerevisiae*. The difference in inhibition constants might be due to temperature differences for the assay as well as difference in the susceptibility to the inhibitors by ODCase from different sources (Table 2).

We reported recently that 6-cyano-UMP is a substrate for ODCase, undergoing very slow conversion into BMP (24−48 h or longer).[17] We were interested in understanding its binding profile to ODCase and its behavior as a competitive inhibitor based on the structural characteristics of the inhibitors. 6-Cyano-UMP indeed exhibited competitive and reversible inhibition of ODCase enzyme activity during the initial phases of the incubation (<1 h). The inhibition was concentration-dependent, with an observable loss of enzyme activity showing characteristic profiles in the thermograms (Figure 4A). Subsequent analyses of the linear regions revealed the inhibition constant as K_i 29 ± 2 μM (Figure 4B,C). A time-dependent assay, measuring the residual enzyme activity as a function of incubation time by isothermal calorimetry, showed an "irreversible" pattern of loss of enzyme activity at two different concentrations of 6-cyano-UMP, 10 and 25 μM (Figure 4D). This pattern was similar to that in our earlier observations.[17] The enzyme lost more than 90% of its activity after 30 h of incubation and did not recover the activity even after 4 days (up to 108 h) of incubation. Conversion of 6-cyano-UMP to BMP is independent of the concentration of the inhibitor in the incubation mixture, and the rates are very similar at two different concentrations, as expected if the concentration of the inhibitor is well above the K_i value (Figure 4E). The time required to inhibit 50% of the enzyme activity ($t_{1/2}$) was estimated to be 5 h (Figure 4E). It should be noted that the "substrate" nature of the 6-cyano-UMP was ignored during the interpretation of 6-cyano-UMP as a competitive inhibitor and it was assumed that the conversion of 6-cyano-UMP to BMP during the 600 s of the assay was negligible. Thus, the above inhibition constant K_i was computed with the assumption that 6-cyano-UMP (**5**) interacted purely as a competitive inhibitor.

6-Amino-UMP (**6**) was similarly assayed as a competitive inhibitor by coinjecting the inhibitor and substrate (Figure 5). This compound showed a typical competitive inhibition profile. The inhibition constant for 6-amino-UMP was determined as 840 ± 25 nM. This molecule does not show any time-dependent loss of activity, eliminating the possibility of covalent interactions.

Several aspects of ITC technique including high sensitivity of the instruments, direct rate measurement, and convenient data analysis make this method attractive to study enzyme inhibitions. Additionally, the requirements for the protein and ligand concentrations are comparable to other techniques commonly used by enzymologists and several orders of magnitude less than a typical ITC thermodynamics experiment. The measurement of the reaction rate is direct and does not require additional coupled reactions. Additionally, these are undisturbed by overlapping absorption characteristics of substrate and inhibitor molecules.

Using ITC, one can determine the inhibition constants for various ODCase inhibitors, and further refinements will make this method a very useful addition to the tool set available to perform enzyme inhibition studies. Additionally, the principles outlined here can be applied to other enzyme systems. In some experiments relatively high concentrations of the inhibitor were used without compromising the quality of measurements. This is not detrimental as long as the energies of interaction between the ligand and the enzyme are negligible in comparison to those of the biochemical reaction. We also report for the first time that 6-amino-UMP (**6**) acts as a nanomolar inhibitor of ODCase and 6-cyano-UMP as a competitive inhibitor. The principles and methods outlined here pave the way for the design of novel ODCase inhibitors and provide new means to investigate enzyme inhibition kinetics.

Acknowledgment. We thank Dr. David Clarke for generously sharing the VP-ITC calorimeter for these experiments. We are grateful to Ms. Wanda Gillon for her expert help with enzyme purification. This work was supported by a grant from the Canadian Institutes of Health Research (E.F.P. and L.P.K.). L.P.K. is a recipient of an Rx&D HRF-CIHR research career award and Premier's Research Excellence award. An infrastructure grant from the Ontario Innovation Trust provides support for the Molecular Design and Information Technology Centre. E.F.P. acknowledges support through the Canada Research Chairs program. M.F. was a recipient of an Overseas Fellowship and a Research Fellowship for young scientists from the Japan Society for the Promotion of Science (JSPS).

Supporting Information Available: Thermograms and isotherms illustrating the titration curves for 5-aza-UMP (**3**) and 6-cyano-UMP (**5**) by use of ODCase enzyme; HPLC and purity data for compounds **5** and **6**; and isotherms of titration with UMP and multiple injections of OMP. This material is available free of charge via the Internet at http://pubs.acs.org.

References

(1) Radzicka, A.; Wolfenden, R. A proficient enzyme. *Science* **1995**, *267*, 90−93.
(2) Reichard, P. The enzymatic synthesis of pyrimidines. *Adv. Enzymol. Mol. Biol.* **1959**, *21*, 263−294.
(3) Donovan, W. P.; Kushnerm, S. R. Purification and characterization of orotidine-5′-monophosphate decarboxylase from *Escherichia coli* K-12. *J. Bacteriol.* **1983**, *156*, 620−624.

(4) Pragobpol, S.; Gero, A. M.; Lee, C. S.; O'Sullivan, W. J. Orotate phosphoribosyltransferase and orotidylate decarboxylase from *Crithidia luciliae*: Subcellular location of the enzymes and a study of substrate channeling. *Arch. Biochem. Biophys.* **1984**, *230*, 285−293.
(5) Warshel, A.; Florian, J. Computer simulations of enzyme catalysis: finding out what has been optimized by evolution. *Proc. Natl. Acad. Sci. U.S.A.* **1998**, *95*, 5950−5955.
(6) Miller, B. G.; Wolfenden, R. Catalytic proficiency: The unusual case of OMP decarboxylase. *Annu. Rev. Biochem.* **2002**, *71*, 847−885.
(7) Kotra, L. P.; Pai, E. F.; Bello, A. M.; Fujihashi, M.; Poduch, E. Inhibitors of orotidine monophosphate decarboxylase (ODCase) activity. U.S. Pat. Appl. 60/596,537,2005.
(8) Levine, H. L.; Brody, R. S.; Westheimer, F. H. Inhibition of orotidine-5′-phosphate decarboxylase by 1-(5′-phospho-β-D-ribofuranosyl)-barbituric acid, 6 azauridine 5′-phosphate, and uridine 5′-phosphate, *Biochemistry* **1980**, *19*, 4993−4999.
(9) Smiley, J. A.; Saleh, L. Active site probes for yeast OMP decarboxylase: Inhibition constants of UMP and thio-substituted UMP analogues and greatly reduced activity toward CMP-6-carboxylate. *Bioorg. Chem.* **1999**, *27*, 297−306.
(10) Gabrielsen, B.; Kirsi, J. J.; Kwong C. D.; Carter, D. A.; Krauth, C. A.; Hanna, L. K.; Huggins, J. W.; Monath, T. P.; Kefauver, D. F.; Blough, H. A.; Rankin, J. T.; Bartz, C. M.; Huffman, J. H.; Smee, D. F.; Sidwell, R. W.; Shannon, W. M.; Secrist, J. A. In-vitro and in-vivo antiviral (RNA) evaluation of orotidine 5′-monophosphate decarboxylase inhibitors and analogues including 6-azauridine-5′-(ethyl methoxyalaninyl)phosphate (a 5′-monophosphate prodrug). *Antiviral Chem. Chemother.* **1994**, *5*, 209−220.
(11) Nord, L. D.; Willis, R. C.; Smee, D. F.; Riley, T. A.; Revankar, G. R.; Robins, R. K. Inhibition of orotidylate decarboxylase by 4(5*H*)-oxo-1-β-D-ribofuranosylpyrazolo[3,4-*d*]pyrimidine-3-thiocarboxamide (APR-TC) in B lymphoblasts. Activation by adenosine kinase. *Biochem. Pharmacol.* **1988**, *37*, 4697−4705.
(12) Smee, D. F.; McKernan, P. A.; Nord, L. D.; Willis, R. C.; Petrie, C. R.; Riley, T. M.; Revankar, G. R.; Robins, R. K.; Smith, R. A. Novel pyrazolo[3,4-*d*]pyrimidine nucleoside analogue with broad-spectrum antiviral activity. *Antimicrob. Agents. Chemother.* **1987**, *31*, 1535−1541.
(13) Morrey, J. D.; Smee, D. F.; Sidwell, R. W.; Tseng, C. Identification of active antiviral compounds against a New York isolate of West Nile virus. *Antiviral Res.* **2002**, *55*, 107−116.
(14) Krungkrai, S. R.; DelFraino, B. J.; Smiley, J. A.; Prupunwattana, P.; Mitamura, T.; Horii, T.; Krungkrai, J. A novel enzyme complex of orotate phosphoribosyltransferase and orotidine 5′-monophosphate decarboxylase in human malaria parasite *Plasmodium falciparum*: Physical association, kinetics and inhibition characterization. *Biochemistry* **2005**, *44*, 1643−1652.
(15) Chen, J. J.; Jones, M. E. Effect of 6-azauridine on de novo pyrimidine biosynthesis in cultured Ehrlich ascites cells. Orotate inhibition of dihydrorotase and dihydroorotase dehydrogenase. *J. Biol. Chem.* **1979**, *254*, 4908−4914.
(16) Cadman, E. C.; Dix, D. E.; Handschumacher, R. E.; Clinical, biological and biochemical effect of pyrazofurin. *Cancer Res.* **1978**, *38*, 682−698.
(17) Fujihashi, M.; Bello, A. M.; Poduch, E.; Wei, L.; Annedi, S. C.; Pai, E. F.; Kotra, L. P. An unprecedented twist to ODCase catalytic activity. *J. Am. Chem. Soc.* **2005**, *127*, 15048−15050.
(18) Kotra, L. P.; Pai, E. F.; Bello, A. M.; Fujihashi, M.; Poduch, E. Inhibitors of orotidine monophosphate decarboxylase (ODCase) activity. U.S. Pat. Appl. 60/596,537, 2005.
(19) Krungkrai, J.; Wutipraditkul, N.; Prapunwattana, P.; Krungkrai, S. R.; Rochanakij, S. A nonradioactive High-Performance Liquid Chromatographic measurement of uridine 5′-monophosphate synthase, orotate phosphoribosyltransferase, and orotidine 5′-monophosphate decarboxylase. *Anal. Biochem.* **2001**, *299*, 162−168.
(20) Wiseman, T.; Williston, S.; Brandts, J. F.; Lin, L. N. Rapid measurement of binding constants and heats of binding using a new titration calorimeter. *Anal. Biochem.* **1989**, *179*, 131−137.
(21) Todd, M. J.; Gomez, J. Enzyme kinetics determined using calorimetry: a general assay for enzyme activity? *Anal. Biochem.* **2001**, *296*, 179−187.
(22) Bianconi, M. L. Calorimetric determination of thermodynamic parameters of reaction reveals different enthalpic compensations of the yeast hexokinase isozymes. *J. Biol. Chem.* **2003**, *278*, 18709−18713.
(23) (a) Wu, N.; Christendat, D.; Dharamsi, A.; Pai, E. F. Purification, crystallization and preliminary X-ray study of orotidine 5′-monophosphate decarboxylase. *Acta Crystallogr.* **2000**, *D56*, 912−914. (b) Wu, N.; Mo, Y.; Gao, J.; Pai, E. F. Electrostatic stress in catalysis: Structure and mechanism of the enzyme orotidine monophosphate decarboxylase. *Proc. Natl. Acad. Sci. U.S.A.* **2000**, *97*, 2017−2022.
(24) *SPARTAN*, version 5.0; Wave function Inc.: Irvine, CA.
(25) Morin, P. E.; Freire, E. Direct calorimetric analysis of the enzymatic activity of yeast cytochrome *c* oxidase. *Biochemistry* **1991**, *30*, 8494−8500.
(26) Origin, Tutorial Guide, Version 7.0, January 2004, 92−93; MicroCal, LLC: Northampton, MA.
(27) Dixon, M. The graphical determination of K_m and K_i. *Biochem. J.* **1972**, *129*, 197−202.
(28) Tanaka, H.; Hayakawa, H.; Haraguchi, K.; Miyasaka, T. Introduction of an azido group to the C-6 position of uridine by the use of a 6-iodouridine derivative. *Nucleosides Nucleotides* **1985**, *4*, 607−612.
(29) Tanaka, H.; Hayakawa, H.; Miyasaka, T. "Umpolung" of reactivity at the C-6 position of uridine: a simple and general method for 6-substituted uridines. *Tetrahedron* **1982**, *38*, 2635−2642.
(30) Sowa, T.; Ouchi, S. Facile synthesis of 5′-nucleotides by selective phosphorylation of a primary hydroxyl group of nucleosides with phosphoryl chloride. *Bull. Chem. Soc. Jpn.* **1975**, *48*, 2084−2090.
(31) Ueda, T.; Yamamoto, M.; Yamane, A.; Imazawa, M.; Inoue, H. Conversion of uridine nucleotides to the 6-cyano derivatives: synthesis of orotidylic acid. *Carbohydr. Nucleosides Nucleotides* **1978**, *5*, 261−271.
(32) Bhatnagar, R. S.; Schall, O. F.; Jackson-Machelski, E.; Sikorski, J. A.; Devadas, B.; Gokel, G. W.; Gordon J. I. Titration calorimetric analysis of acylCoA recognition by myristoylCoA:protein N-myristoyltransferase. *Biochemistry* **1997**, *36*, 6700−6708.
(33) Bougie, I.; Parent, A.; Bisaillon, M. Thermodynamics of ligand binding by the yeast mRNA-capping enzyme reveals different modes of binding. *Biochem. J.* **2004**, *384*, 411−420.
(34) Fak, J. J.; Itkin, A.; Ciobanu, D. D.; Lin, E. C.; Song, X. J.; Chou, Y. T.; Gierasch, L. M.; Hunt J. F. Nucleotide exchange from the high-affinity ATP-binding site in SecA is the rate-limiting step in the ATPase cycle of the soluble enzyme and occurs through a specialized conformational state. *Biochemistry* **2004**, *43*, 7307−7327.
(35) Moore, J. L.; Gorshkova, I. I.; Brown, J. W.; McKenney, K. H.; Schwarz, F. P. Effect of cAMP binding site mutations on the interaction of cAMP receptor protein with cyclic nucleoside monophosphate ligands and DNA. *J. Biol. Chem.* **1996**, *271*, 21273−21278.
(36) Microcal VP-ITC Microcalorimeter User's Manual, p 38.
(37) Brown, G. K.; Fox, R. M.; O'Sullivan, W. J. Interconversion of different molecular weight forms of human erythrocyte orotidylate decarboxylase. *J. Biol. Chem.* **1975**, *250*, 7352−7358.
(38) Donovan, W. P.; Kushnerm, S. R. Purification and characterization of orotidine-5′-phosphate decarboxylase from *Escherichia coli* K-12. *J. Bacteriol.* **1983**, *156*, 620−624.
(39) Pragobpol, S.; Gero, A. M.; Lee, C. S.; O'Sullivan, W. J. Orotate phosphoribosyltransferase and orotidylate decarboxylase from *Crithidia luciliae*: subcellular location of the enzymes and a study of substrate channeling. *Arch. Biochem. Biophys.* **1984**, *230*, 285−293.
(40) Wolf-Watz, M.; Thai, V.; Henzler-Wildman, K.; Hadjipavlou, G.; Eisenmesser, E. Z.; Kern, D. Linkage between dynamics and catalysis in a thermophilic-mesophilic enzyme pair. *Nat. Struct. Mol. Biol.* **2004**, *11*, 945−949.
(41) Miller, B. G.; Butterfoss, G. L.; Short, S. A.; Wolfenden, R. Role of enzyme−ribofuranosyl contacts in the ground state and transition state for orotidine 5′-phosphate decarboxylase: a role for substrate destabilization? *Biochemistry* **2001**, *40*, 6227−6232.
(42) Miller, B. G.; Snider, M. J.; Short, S. A.; Wolfenden, R. Contribution of enzyme−phosphoribosyl contacts to catalysis by orotidine 5′-phosphate decarboxylase. *Biochemistry* **2000**, *39*, 8113−8118.

JM060202R